HHS Public Access

Author manuscript

J Cancer Stem Cell Res. Author manuscript; available in PMC 2015 February 19.

Published in final edited form as:

J Cancer Stem Cell Res. ; 2014(2): . doi:10.14343/JCSCR.2014.2e1003.

T_{reg}/Th17 polarization by distinct subsets of breast cancer cells is dictated by the interaction with mesenchymal stem cells

Shyam A. Patel[1,2], **Meneka A. Dave**[1], **Sarah A. Bliss**[1,2], **Agata B. Giec-Ujda**[1,2], **Margarette Bryan**[1], **Lillian F. Pliner**[1], and **Pranela Rameshwar**[1]

[1]Dept of Medicine, Hematology/Oncology, New Jersey Medical School, Rutgers School of Biomedical Health Sciences, Newark, NJ, USA

[2]Graduate School of Biomedical Sciences, Rutgers School of Biomedical Health Sciences, Newark, NJ, USA

Abstract

Breast cancer (BC) cells (BCCs) exist within a hierarchy beginning with cancer stem cells (CSCs). Unsorted BCCs interact with mesenchymal stem cells (MSCs) to induce regulatory T cells (T_{regs}). This study investigated how distinct BCC subsets interacted with MSCs to polarize T-cell response, T_{regs} versus T helper 17 (Th17). This study tested BC initiating cells (CSCs) and the relatively more mature early and late BC progenitors. CSCs interacted with the highest avidity to MSCs. This interaction required CXCR4 and connexin 43 (Cx43)-dependant gap junctional intercellular communication (GJIC). This interaction induced T_{reg} whereas interactions between MSCs and the progenitors induced Th17 response. The increases in T_{reg} and Th17 depended on MSCs but not CTLA-4, which was increased in the presence of MSCs. Studies with BM stroma (fibroblasts) and MSCs from the same donors, indicated specific effects of MSCs. In total, MSC-CSC interaction required CXCR4 for GJIC. This led to increased T_{regs} and TGFβ, and decreased Th17. In contrast, late and early BCCs showed reduced formation of GJIC, decreased T_{reg} and increased Th17 and IL-17. These findings have significance to the methods by which CSCs evade the immune response. The findings could provide methods of intervention to reverse immune-mediated protection and support of BC.

INTRODUCTION

The heterogeneity of tumors has led to intensive research to identify the cancer initiating cells referred as cancer stem cells (CSCs). The past few years have seen a surge of articles in the literature on CSCs and mesenchymal stem cells (MSCs). Together, these fields have converged within the area of cancer immunology. The literature mostly reported on the immune response to a heterogeneous population of cancer cells. It is unclear if each cancer cell subset elicits a distinct immune response. This question is important because answers would provide information on the method by which dormant cancer stem cells evade the

Correspondence: Pranela Rameshwar, Ph.D., Department of Medicine – Division of Hematology/Oncology, New Jersey Medical School, Rutgers School of Biomedical Health Science, Newark, NJ 07103 USA; rameshwa@njms.rutgers.edu.

immune response. Similarly, there is little information on the effect of a microenvironment on the immune response to distinct subset of cancer [1].

Breast cancer (BC) continues to lead as the most common cancer among women in the United States and the second leading cause of cancer-related death. Immune dysfunctions occur in patients with cancer [1, 2]. This has led to decades of research to determine how immune therapy can be applied to boost the immune system to respond to cancer. Based on the outcome of these studies, it is evident that such therapy faces numerous challenges. For example, MSCs can support tumor growth and also suppress the immune response [3, 4]. Additionally, MSCs can also exert immune enhancing properties [5]. Thus, it is unclear how MSCs respond at a particular time of progression of the tumor. The discussions in this paragraph underscores the complex issues to overcome immune therapy [6].

MSCs are multipotent cells that can generate specialized cells of all germ layers [7, 8]. MSCs are ubiquitous and are referred by different names such as pericytes [9]. Although MSCs can be found in multiple tissues, they are phenotypically similar but seem to exert varied functions, depending on the source. MSCs are desirable stem cells for therapy mostly because of ease in expansion, reduced ethical concerns and low probability of transformation [8, 10]. MSCs can support cancer survival by protecting them from the immune responses, and by supporting their growth [4, 11–19]. Taken together, the properties of MSCs could lead to a complex cellular relationship with cancer cells.

Interaction between MSCs and unsorted BC cells (BCCs) increased regulatory T-cells (T_{regs}) [11]. This study applied a working hierarchy of BCCs [20] to determine how interactions between MSCs and CSCs or non-CSCs affect T-cell outcomes, T_{reg} versus T-helper (Th17). T_{reg}/Th17 differentiation is balanced during T-cell development, and is influenced by the local cytokine milieu [21, 22]. Th17 can be differentiated from FoxP3(+) naïve T_{regs} within a cytokine milieu of IL-1β, IL-2, IL-23, and TGF-β [23].

IL-6 and transforming growth factor-β (TGF-β) governs the differentiation of T-cells to T_{reg} or Th17. IL-6 mediates the differentiation of naïve CD4(+) T-cells by inhibiting the development of T_{regs} and promoting Th17 differentiation for anti-tumor response [22]. The role of Th17 in cancer is not limited to one type of malignancy. Th17 and the production of the associated cytokines, IL-17 and IL-23, have been reported in human glioma [24].

TGF-β can induce the differentiation of both T-cell subsets including the differentiation within a tumor micro-environment, promotes tumor growth and angiogenesis during the late stage of cancer, inhibits tumor cell proliferation during the early stage through inhibitors of cyclin-dependent kinases (Cdk) [25].

During the early stages of cancer, the frequency of Th17 cells was relatively high as compared to the more advanced stages when there was a switch to T_{regs} [26]. Cervical cancer with vascular invasion and lymph node metastasis have higher levels of Th17 cells as compared to T_{regs} [27]. Together, these findings suggested that the early phase of cancer is accompanied by a predominance of Th17 to facilitate initial invasion and tumor growth. In contrast, T_{reg} accumulation at the later stages might serve to protect the tumor cells by

contributing to immune subversion [26]. In other studies, MSCs have been shown to increase T_{regs} [11].

In other studies, IL-17F inhibited the growth of gastric cancer [28]. Similarly, an analysis of the microenvironment of IL-17-transfected colon cancer cells revealed a decrease in VEGF levels and CD31(+) cells [28]. Thus, Th17 cells appeared to exert a bimodal role with regards to the functions on cancer, hence the need to dissect its induction in BC.

Due to the heterogeneity of BCCs, the question is whether the bimodal role of Th17 could be explained by distinct BCC subsets and/or the microenvironment. To this end, we proposed that the key to dormancy resides in the interaction between specific components of the immune microenvironment and particular cellular subsets of BCCs. This question was studied with CSCs and non-CSCs, referred as BC progenitors.

Our findings showed high avidity interaction between CSCs and MSCs with polarized T_{regs}. The interaction between CSCs and MSCs resulted in gap junctional intercellular communication (GJIC). The formation of GJIC required an initial interaction between membrane CXCR4 and CXCL12. In contrast, BC progenitors and MSCs resulted in Th17. The effects of MSCs were specific since fibroblasts could not show a similar effect with regards to T-cell polarization. The findings are discussed in the context of cancer progression, immune subversion and dormancy in bone marrow.

MATERIALS AND METHODS

Reagents

DMEM and α-MEM were purchased from Gibco (Grand Island, NY), premium fetal calf serum from Hyclone Laboratories (Logan, UT), another source of Ficoll-Hypaque, RPMI 1640, AMD3100 and carbenoxolone from Sigma (St. Louis, MO), Vybrant CFDA-SE cell tracer and geneticin G418 from Invitrogen (Carlsbad, CA), brefeldin from eBioscience (San Diego, CA), restore western blot stripping buffer and NE-PER Nuclear and Cytoplasmic Extraction Kit from Thermo Scientific (Waltham, MA), HyGLO HRP Chemiluminescent Detection Kit from Denville Scientific (Metuchen, NJ) and, effectene transfection reagent from QIAGEN (Valencia, CA).

Antibodies and cytokines

Human Regulatory T Cell Staining Kit and Human Th17 Staining Panel were purchased from eBioscience (San Diego, CA). Platinum Taq polymerase, connexin sampler pack antibodies, Platinum SYBR Green qPCR SuperMix-UDG Kit, and SuperScript III reverse transcriptase were purchased from Molecular Probes-Invitrogen (Carlsbad, CA); Texas Red-X phalloidin from Molecular Probes (Eugene, OR); donkey anti-rabbit IgG-FITC and APC-anti-rabbit IgG, mouse anti-CTLA-4 (F8) were purchased from Santa Cruz Biotechnology, Inc. (Santa Cruz, CA); 4′-6′-diamidino-2-phenylindole nuclear stain (DAPI), mouse monoclonal IgG to β-actin, mouse anti-β-actin mAb; rabbit polyclonal anti-CXCR7, were purchased from Abcam (Cambridge, MA); horse anti-mouse IgG-HRP from Cell Signaling (Denvers, MA); human TGF-β1 and rabbit neutralizing Ab to TGF-β1 were purchased from R&D Systems (Minneapolis, MN).

Cell lines

MDA-MB-231 (highly invasive, basal-like) and T47D (low-invasive, luminal) were purchased from American Type Culture Collection (ATCC) and cultured as per manufacturer's instructions. CCL64 cell line was previously described [29].

Vectors

HuSH 29mer *GJA1* (Cx *GJA1* 43) shRNA, ligated in pRFP-C-RS, and vector alone were purchased from Ori-Gene Technologies (Rockville, MD). pSUPER-CXCR4 (wild-type and mutant) shRNA vector were kindly provided by Dr. Si-Yi Chen (Baylor University),

Cell Adhesion Assay

Adhesion of BCCs to MSCs was studied as described [18] with the Cell Adhesion Assay Kit (Invitrogen. MSCs (10^4/well) were added to 96-well plates. After 24 h, 10^3 BCCs were labeled with the fluorescent cytoplasmic tracer, Vybrant CFDA SE and then added to the confluent MSC. Non-specific binding was studied in wells without MSCs. After 15 min, the non-adherent cells were washed twice with PBS and the adherent cells were detected by fluorescence on the FL1500 Fluorescent Microplate Reader (Biotek, Winooski, VT). Non-specific adherence was subtracted from the test wells.

Human subjects

The use of human subjects was approved by the Institutional Review Board at Rutgers, Newark Campus, NJ. All subjects signed the informed consent. Peripheral blood (PB) and bone marrow (BM) aspirates were obtained from healthy volunteers ranging between 18 and 35 years. Mononuclear cells were isolated from the PB (PBMCs) by Ficoll-Hypaque gradient and then cryopreserved until the MSCs were ready for use in the functional assays. BM aspirates were used to culture MSCs and stromal cells.

TGF-β1 and IL-17 quantitation

Bioactive TGF-β1 was performed as described [29]. Briefly, CCL64 cells were seeded in 24-well culture plates and culture supernatant added after adherence of cells. After 72 h, growth inhibition was determined by counting viable cells. TGF-β1 levels were determined in a standard curve established with known concentrations of the cytokine. The specificity was determined by repeating assays with neutralizing anti-TGF-β1 at 1.0 pM.

IL-17 was quantitated using a tissue culture kit from Meso Scale Discovery (Rockville, MD). The assay followed manufacturer's instructions. The data are presented as fold change over the baseline produced by PBMC alone.

Culture of mesenchymal stem cell (MSC)

MSCs were cultured from BM aspirates, as described [30]. Briefly, unfractionated aspirates were diluted in DMEM and then added to vacuum gas plasma-treated plates (BD Falcon; Franklin Lakes, NJ). After 3 days, red blood cells and granulocytes were removed by Ficoll-Hypaque density gradient centrifugation and the mononuclear fraction was replaced. At weekly intervals, 50% of the media was replaced with fresh media. The adherent cells were

serially passage five times after the growth attained ~80% confluence. After four cell passages, the adherent cells were symmetric, CD14–, CD29+, CD44+, CD34–, CD45–, CD105+ prolyl-4-hydroxylase–.

Culture of BM stroma (fibroblasts)

BM stromal cells were cultures as described [31, 32]. Briefly, BM aspirates were incubated with stromal culture medium, which consisted a minimal essential medium (α-MEM) with 12.5% FCS, 12.5% horse sera, 0.1 mM hydrocortisone, 0.1 mM 2-mercaptoethanol and 1.6 mM glutamine. After 3 days, the mononuclear cells were selected by Ficoll-Hypaque density-gradient centrifugation and then replaced in fresh stromal media. Fifty percent of the media were replaced weekly until 80% confluence. Trypsinized adherent cells were passaged at least five times to be used as in the cellular immune assays.

Isolation of BCC subsets

BCC subsets were selected from MDA-MB-231 and T47D, stably transfected with pEGFP1-Oct3/4 as described [20]. Briefly, the stable transfectants were maintained in G418, and the cells were sorted with the FACSDiva (BD Biosciences), based on the intensity of GFP. The top 5%, which we previously shown to contain the initiating cells (CSC) [20]. The lower 5%, which we previously shown to be late progenitors were selected in addition to those with medium expression of *Oct4*, which were designated early progenitors [20].

Gap Junctional Intercellular Communication (GJIC)

Two methods were used to study GJIC using dye transfer by microscopic method and by flow cytometry as described [20, 33]. BCC subsets were selected as described [20] and then labeled with CFDA-SE cell tracer. The BCCs were co-cultured with MSCs at 1:1 ratio. After 48 h, the cultures were washed with PBS and then examined for dye transfer to the MSCs using the AMG EVOS*fl* fluorescent imager and also by flow cytometry. The specificity of GJIC was studied in the presence of 200 μM carbenoxolone.

Intercellular adherence between BCCs and MSCs

The effects of CXCR4 in intercellular adhesion between BCCs and MSCs were studied by pharmacological and molecular methods. The former used 100 ng/ml AMD3100 or vehicle whereas the latter stably knockdown CXCR4 in BCCs with pSUPER-CXCR4 (wild-type and mutant) shRNA vector, also previously described [34]. BC-ICs were selected from the CXCR4 knockdown cells within the top 5% of GFP (+) cells, described above [20]. The selected cells were immediately analyzed for GJIC with MSCs.

Flow cytometry for T_{regs} and Th17 responses

PBMCs were isolated from PB by Ficoll Hypaque density gradient and then analyzed by flow cytometry for Th17 and T_{reg} using specific markers. The cells were labeled with Human Th17 and T_{reg} staining panels. PBMCs were cultured with BCC subsets in the presence or absence of MSCs (50:1 ratio of PBMCs:BCCs; 1:1 ratio of BCCs:MSCs). Co-cultures were maintained at 37°C. At day 5, the PBMCs were harvested, fixed in 2%

paraformaldehyde, permeabilized and then incubated in Brefeldin for intracellular cytokine staining. The Brefeldin retained intracellular cytokines for detection by flow cytometry.

The cells were incubated in FITC-anti-IL-17A, PE-anti-IL-17F, PerCP-anti-IL-22, and eFluor660-anti-IL-21 for 30 min at 4°C. The cells were washed in PBS, and Th17 acquisition was done by gating on the CD4(+) population. The data were analyzed with CellQuest software (BD Biosciences).

Labeling for T_{regs} used the Human Regulatory T Cell Staining Kit, which includes FITC-anti-CD4, APC-anti-CD25 and PE-anti-FoxP3. Briefly, PBMCs were cultured with BCC subsets in the presence or absence of MSCs (50:1 ratio of PBMCs:BCCs, 1:1 ratio of BCCs:MSCs). Co-cultures were maintained for 5 days at 37°C. After PBMC isolation via gradient centrifugation, PBMCs were cell surface-stained for CD4 and CD25 for 30 min at 4°C, then permeabilized, then stained for FoxP3 for 30 min at 4°C. Cells were washed in PBS, and analyses were performed using the FACSCalibur system (BD Biosciences). Cells were gated on the CD4(+) population prior to acquisition of CD25 and FoxP3 emissions. PE-rat IgG2a isotype was used as control for PE-FoxP3 emissions.

Real-time PCR

RNA extraction was performed via RNeasy Mini Kit from (Qiagen, Valencia, CA). Total RNA (1 μg) were immediately reverse transcribed using dNTPs (0.2 mM), random hexamers (50 μM), and SuperScript III reverse transcriptase (200 U). Incubation conditions were, 25°C for 5 min, 50°C for 60 min, and 70°C for 15 min. Real-time PCR was performed with 200 ng cDNA using Platinum SYBR Green qPCR SuperMix-UDG Kit (Invitrogen) and then analyzed on the 7300 Real-Time PCR System (Applied Biosystems, Foster City, CA). The analyses were performed with an initial incubation of 50°C for 2 min followed by 95°C for 2 min. After this, the cycling conditions were as follows: 94°C for 15 sec and 60°C for 45 sec, for 40 cycles. The primer sequences for CXCR4 were: F: 5′-CTT GTG GGT GGT TGT GTT- 3′; R: 5′-GAA AGC CAG GAT GAG GAT-3′. The values obtained for late BC progenitors were assigned 1 and then used to present the fold changes in CSCs.

Western Blot

Whole cell extracts were isolated with M-PER Mammalian Protein Extraction Reagent or the Cytoplasmic/Nuclear NE-PER reagent (Thermo Scientific, Danvers, MA). The extracts (10 μg) were analyzed by western blots on 12% SDS-PAGE gels (Bio-Rad, Hercules, CA). Proteins were transferred onto PVDF membranes (Perkin Elmer, Boston, MA). The membranes were incubated overnight with primary antibodies at a final dilution of 1/500 followed by 2 h incubation with HRP-conjugated IgG at 1/2000 final dilution. HRP activity was detected by chemiluminescence using SuperSignal West Femto MaximumSensitivitySubstrate(ThermoScientific).MembraneswerestrippedwithRestoreStrippingBuffer(Thermo Scientific) prior to reprobing with other antibodies.

Statistical analyses

Data were analyzed using the paired t-test for two comparable groups (control vs experimental). A p value <0.05 was considered significant.

RESULTS

Relative T_{reg} in co-cultures with MSCs and BCC subsets

MSCs can be recruited to cancer cells where they contribute to immune subversion [20, 35, 36]. We previously reported on a 2-fold induction of T_{regs} when MSCs were co-cultured with unsorted BCCs [20]. Due the heterogeneity among BCCs, it was unclear if the increase in T_{reg} was caused by a particular BCC subset. This study co-cultured PBMCs, MSCs, and different BCC subsets. After 5 days, we analyzed the CD4+ cells (Figure 1, top panel) for T_{reg} by analyzing for FoxP3 and CD25.

CSCs showed a significant increase in T_{regs} as compared to late and early BC progenitors (Figure 1, left panels). MSCs did not affect ($p > 0.05$) the percentage of T_{regs} when co-cultured with of late and early BC progenitors (Figure 1, first and second panels). In contrast, the presence of MSCs and CSCs caused a significant ($p < 0.05$) increase in T_{regs} (Figure 1, third panels). Overall, the results showed preferential increase in T_{regs} with CSCs, with further increase in the presence of MSCs. Also, the induction of T_{regs} was directly proportional to the relative maturity of BCCs.

Relative Th17 induction in co-cultures with MSCs and BCC subsets

Since T_{reg} and Th17 exist in a delicate balance, we studied the relative levels of Th17 in co-cultures of PBMCs, MSCs and different BCC subsets as described for Figure 1. At day 5, the cells were analyzed by flow cytometry. The CD4 (+) cells were analyzed for IL17A, IL-17R and IL-22 (Figure 2). There were significant ($p < 0.01$) increases in IL-17F when the co-cultures contained BC progenitors (last row-middle panels) as compared to baseline/ PBMCs alone (left panels) and CSCs (right panels). Similar analyses for IL-17A showed no difference (second row -middle panels).

IL-22, a Th17-associated cytokine, was also significantly ($p < 0.05$) elevated in the early and late progenitors as compared CSCs and PBMCs alone (rows 2 and 3/ upper quadrants). The percentages of IL-17F/IL-22 (last row, right quadrants) were 2-fold higher with BC progenitors as compared to CSCs. In summary, the results showed increases of IL-22- and IL-17F-producing CD4+ cells with MSCs and BC progenitors as compared to CSCs.

CTLA-4 in PBMCs from co-cultures with or without MSCs

The presence of MSCs and distinct BCC subset induces T_{regs} or Th17 (Figures 1 and 2). We asked if this could be explained by the inhibitory molecule T-cell activation, CTLA-4. The PBMCs from the co-cultures were selected by negative depletion of MSCs with anti-CD105 and then studied for CTLA-4 by western blots with whole cell extracts. The cultures containing MSCs showed increases in bands for CTLA-4 as compared to similar cultures without MSCs (Figure 2B). The presence of CTLA-4 was independent of the BCC subtype, indicating that the T-cell responses shown in Figures 1 and 2A did not depend on CTLA-4.

Th17 and TGFβ1 levels in co-cultures with different BCC subsets

Since the relative levels of Th17 and T_{regs} depended on the particular BCC subset (Figures 1, 2), we asked if this finding correlated with the associated differentiating cytokines, IL-17

and TGFβ1. We co-cultured PBMCs with different BCC subsets, with or without MSCs. After 3 days, the media were collected and then studied for Th17 by ELISA and bioactive TGFβ1. The cytokines were presented as fold change over baseline (PBMC alone).

MSCs and BC progenitors caused a significant ($p < 0.01$) increase in IL-17 as compared to CSCs (Figure 3A, left group). IL-17 was also increased with early BC progenitors alone, although the levels were was significantly ($p < 0.01$) reduced as compared to similar cultures with MSCs (Figure 3A, right group vs. left group). Analyses, similar to those for IL-17, were performed for TGFβ (Figure 3B). TGFβ level was significantly increased in cultures with CSCs and MSC as compared to BC progenitors and MSCs (Left group). In the absence of MSCs, CSCs caused a significant increase in TGFβ as compared to parallel cultures with BC progenitors but significantly less significant less than cultures with MSCs (Figure 3B right vs. left group). Together, MSCs caused significant increases in IL-17 and TGFβ productions in cultures with BC progenitors and CSC respectively.

Specific interaction between MSCs and distinct BCC subset

In order to explain why distinct BCC subset and MSCs resulted in a particular T-cell type, we studied their cellular interactions. The avidity between MSCs and CSC or late BC progenitors was studied with a fluorescence-based adherence assay. The BCC subsets were selected from MDA-MB-231 and T47D as described [20]. MSCs showed significantly ($p < 0.05$) higher avidity for CSCs as compared to unsorted and late progenitor BCCs (Figure 4A).

We next asked it the preferential interaction between CSCs and MSCs could be due to gap junctional intercellular communication (GJIC). A similar interaction was reported for CSCs and differentiated MSCs (bone marrow stroma) [20]. GJIC was studied with dye exchange studies and dye transfer was assessed by flow cytometry and fluorescence microscopy, as described [31, 33]. The results from both methods were similar and are therefore presented together as % GJIC frequency. There was a significant ($p < 0.01$) increase in GJIC with CSCs as compared to BC progenitors (Figures 4B, S1). The early BC progenitors, which is relatively more immature than the late progenitors [20] showed a significantly ($p < 0.05$) higher frequency of GJIC (Figure 4B). Parallel studies with 200 μM carbenoxolone blocked dye transfer, indicating specific dye exchange through GJIC (Figure S1). In summary, the most immature CSCs showed the highest avidity for MSCs and this correlated with GJIC between the two cell types.

Role of *Cx43* in GJIC between MSCs and CSC

We previously reported on the expression of *Cx32* and *Cx43* on CSCs [20]. Since the Cxs are required for GJIC we performed western blots to identify the type of Cxs on MSCs. Western blots were performed for Cx43 and Cx32 with whole cell extracts from MSCs and BCCs (unsorted, progenitors and CSCs). Both Cxs were detected in CSCs and MSCs (Figure 5A). Cx32 was not detected with the extracts from BCC progenitors (Figure 5A). Double bands for Cx43 were noted with extracts from CSCs, suggesting phosphorylation of the active form [33].

Since Cx43 was identified on both CSCs and MSCs we asked if it was required for GJIC. This was addressed with *Cx43* knockdown CSCs. We compared different shRNA sequences and identified shRNA 77 as the most efficient (Figure 5B). Dye exchange studies for GJIC with MSCs and CSCs were performed. The CSCs were knockdown for *Cx43* or transfected with a non-targeting shRNA. The results showed a significant ($p < 0.01$) decrease in GJIC with the Cx43 knockdown CSCs as compared with the non-targeting shRNA (Figure 5C), indicating a requirement for Cx43 in GJIC between CSCs and MSCs.

Role of CXCR4 in GJIC between CSCs and MSCs

The interaction between unsorted BCCs and MSCs involved interaction between membrane CXCR4 and CXCL12 [18, 34, 37]. We therefore asked if CXCR4 was important for GJIC between MSCs and CSCs. This question was based on the premise that the initial interaction between MSCs and CSCs could occur by a 'tethering' cellular interaction through CXCR4 and CXCL12.

The first set of studies used pharmacological method to determine the role of CXCR4 in the adherence between MSCs and, unsorted BCCs, CSCs and late BC progenitor. CXCR4 was blocked with AMD3100. The adherence of each BCC subset was significantly ($p < 0.01$) decreased with AMD3100 as compared to vehicle (Figure 6A). The decrease for CSCs was ~5-fold as compared to ~2 fold for unsorted BCCs and late BC progenitors. Next, we determined if AMD3100 prevented GJIC between CSCs and MSCs (Figure 4B). AMD3100 caused a significant ($p < 0.01$) decrease in GJIC as compared to vehicle (Figure 6B).

Real time PCR for CXCR4 indicated ~4 fold more mRNA in CSCs as compared to BC progenitors (Figure 6C). Since CXCL12 can also interact with CXCR7, we studied the expression of CXCR7 on CSCs and then compared with unsorted BCCs [38]. Western blots for CXCR7 showed an undetectable band with extract from CSCs (Figure 6D). We next studied the surface expression of CXCR4 and CXCR7 on CSCs by 2-color flow cytometry. The CSCs were selected by gating the subset with the highest expression of *Oct4* (Figure 3E, top 5%/left panel) as described [20]. The results showed undetectable CXCR7 and 85% cells expressing CXCR4 (Figure 6E, right panel). These results indicated that CSCs expressed CXCR4.

The effect of a pharmacological inhibitor indicated that CXCR4 was involved in GJIC between MSCs and CSCs (Figure 6B). We verified this finding by molecular method with CSCs, knocked down for *CXCR4*. Dye exchange studies showed a significant ($p < 0.01$) decrease in GJIC with the *CXCR4* knockdown CSCs as compared to non-targeting shRNA (Figures 6F and S2). Together, the results showed a role for CXCR4 in GJIC between MSCs and CSCs.

Specificity of MSC-mediated effect on T-cell response

We studied the specificity of MSCs on T-cell response by repeating the co-culture method with differentiated MSCs, stroma (fibroblasts). PBMCs were co-cultured with different BCC subsets and MSCs or bone marrow stroma. The CD4+ cells were then analyzed for the expressions of Fox P3 and IL-17F as indicators of T_{regs} and Th17, respectively (Figures 1,

2). The expressions of Fox P3 and IL17A in cultures with MSCs were negated when the MSCs were replaced with stroma (Figure 7A). A summary of seven different experiments, with MSCs or stroma (fibroblasts) is shown as a bar graph (Figure 7B). The results indicated that the changes in Th17 and T_{reg} in co-cultures were specific to MSCs since bone marrow stroma did not show a similar effect.

Effect of Cx43 and CXCR4 in T-cell responses

Since the results indicated roles for Cx43 and CXCR4 in MSC-BCC interaction, we determined if these two molecules are important for the increases in Th17 and T_{reg}. Co-cultures were established with MSCs and different BCCs, knockdown for *Cx43* or *CXCR4*. After 4 days, the PBMCs were studied for IL17F and Fox P3 by 2-color flow cytometry. The knockdown cells showed minimal expression of IL17F and Fox P3 (Figure 7C). This contrasted parallel studies with a non-targeting shRNA resulted, which resulted in outcomes similar to Figure 8A (right panels). Together these studies indicated a role for CXCR4 and Cx43 in the induction of T_{regs} in the presence of CSCs and MSCs.

DISCUSSION

This study reported on methods by which BCC heterogeneity could influence the immune microenvironment to achieve distinct T-cell responses. The major findings are summarized in Figure 7D, which showed high avidity interactions between MSCs and CSCs through CXCR4, which led to GJIC. Pharmacological and molecular methods validated a role for CXCR4 in the interaction between CSCs and MSCs for T_{reg}. The role of CXCR4 in the polarization of T-cell response to Th17 was indicated by pharmacological methods. The studies also indicated a yin yang type of T-cell response. Increased T_{reg} was correlated with decreased Th17. The polarized T-cell responses shown in this study while dictated by MSCs, was independent of CTLA-4 (Figure 2B).

The relevance of this report to BC biology is appreciated when considering that both cellular and soluble factors within a tumor microenvironment can dictate cancer growth and chemoresistance. The delineation of T-cell profiles in the context of BC metastasis would lead to an understanding of how BCCs survive as dormant cells and, what how metastasis could be supported. The imbalance in Th17/T_{reg} axis can facilitate tumor dormancy or tumor progression. An intervention of this axis through pharmacological or cell-based therapeutics might reverse and also prevent dormancy. If so, this will eliminate or prevent the eventual tumor resurgence [27]. It is important to recognize the heterogeneity in the expression of key cytokines by T_{regs} and Th17 cells. For example, IL-17 can be produced by naïve T_{regs} and FoxP3 by Th17 cells [24].

Our studies demonstrated important findings in the context of BC metastasis to the BM and provided mechanistic insights regarding previous findings from our laboratory [20]. We propose that, in the BM microenvironment, CSCs come into close contact with MSCs, partly through CXCL12/CXCR4 interaction [18, 34]. GJIC between CSCs ($Oct4^{hi}$ BCCs) and MSCs allows the CSCs to maintain dormancy. Such cellular crosstalk alters T-cell profiles so that immune subversion prevails. The high frequency of T_{regs}, presumably induced by MSC-derived TGF-β1, is likely to protect the CSCs from the immune surveillance system.

This will allow the BCCs to survive and establish dormancy in the BM [11, 20]. Meanwhile, BC progenitors induced a Th17 response (Figure 2), which might be responsible to induce the proliferation of BC progenitors. This point is important because the opposite effect could occur between T_{regs} and CSCs, resulting in their protection until the BCCs reaches the endosteal region where they adapt dormancy [20, 31].

The use of bone marrow stroma (fibroblast) indicated that the effects on T-cell response were specific (Figure 7). The findings provided insights on BC dormancy since the MSCs are components of the hematopoietic niche, including the areas of reduced vascularity close to the endosteum [39]. Since BC dormancy is likely to be within this region, these findings strongly suggested that the protection might occur as the BCCs could traverse the cavity towards the endosteum.

Results from this study and from previous studies in our laboratory highlight the multi-step process of establishing BC dormancy: this process includes chemoattraction of BCC subsets to MSCs, formation of gap junctions, and the maintenance of quiescence through miRNA exchange between BCCs and bone marrow stroma [31]. However, the multi-step nature of establishing dormancy also offers optimistic outlook in that various stages are therapeutically targetable. CXCR4 antagonism, for example, has played a key role in diverting the establishment of dormancy for BCCs and leukemic blasts [34, 40]. CXCR4 antagonists have shown efficacy in promoting chemosensitivity *in vitro* and this information is translated to patients [34, 40]. Another targetable step is the immune microenvironment, namely the T_{reg}/Th17 imbalance that perpetuates dormancy of CSCs while allowing proliferation of BC progenitors. Finally, characterization of individual BCC subsets, such as those with stem-like properties, can lead to identification of targetable phenotypes that will enhance selective depletion of these cells.

Further studies will explore the role of other T-cell subsets and to understand their contribution to BC dormancy, such as Th9 and Th22. These subsets are significant because TGF-β, which is found at varying levels in the tumor microenvironment, has bimodal effects on Th9 and Th22 subsets [25]. Additional studies should also focus on IL-6-based immunotherapeutics, since this cytokine is a key molecular switch that tips the T_{reg}/Th17 axis [41]. By gaining a better understanding of the tri-directional interaction among cancer cells, Th17 cells, and T_{regs}, and the heterogeneity within both T-cell subsets and BCC subsets, one can work towards the development of targeted immune-based therapy for cancer.

ACKNOWLEDGMENTS

The authors thank the flow cytometry core for the input on the analyses of GJIC and T-cell responses. This work was supported by an award given by the Department of Defense, W81XWH-11-1-0276.

REFERENCES

1. Jain RK. Normalizing tumor microenvironment to treat cancer: Bench to bedside to biomarkers. J Clinc Oncol. 2013; 31:2205–18.
2. Sathish JG, Sethu S, Bielsky MC, et al. Challenges and approaches for the development of safer immunomodulatory biologics. Nat Rev Drug Discov. 2013; 12:306–24. [PubMed: 23535934]

3. Dazzi F, Marelli-Berg F. Mesenchymal stem cells for graft-versus-host disease: Close encounters with T cells. Eur J Immunol. 2008; 38:1479–82. [PubMed: 18493977]
4. Momin EN, Vela G, Zaidi HA, et al. The oncogenic potential of mesenchymal stem cells in the treatment of cancer: Directions for future research. Curr Immunol Rev. 2010; 6:137–48. [PubMed: 20490366]
5. Chan JL, Tang KC, Patel AP, et al. Antigen-presenting property of mesenchymal stem cells occurs during a narrow window at low levels of interferon-γ|. Blood. 2006; 107:4817–24. [PubMed: 16493000]
6. Nahas GR, Patel SA, Bliss SA, et al. Can breast cancer stem cells evade the immune system? Curr Med Chem. 2012; 19:6036–49. [PubMed: 22963570]
7. Giordano A, Galderisi U, Marino IR. From the laboratory bench to the patient's bedside: An update on clinical trials with mesenchymal stem cells. J Cell Physiol. 2007; 211:27–35. [PubMed: 17226788]
8. Helmy KY, Patel SA, Silverio K, et al. Stem cells and regenerative medicine: accomplishments to date and future promise. Ther Deliv. 2010; 1:693–705. [PubMed: 21113422]
9. Caplan AI. All MSCs are pericytes? Cell Stem Cell. 2008; 3:229–30. [PubMed: 18786406]
10. Greco SJ, Rameshwar P. Mesenchymal stem cells in drug/gene delivery: implications for cell therapy. Ther Deliv. 2012; 3:997–1004. [PubMed: 22946432]
11. Patel SA, Meyer JR, Greco SJ, et al. Mesenchymal stem cells protect breast cancer cells through regulatory T cells: Role of mesenchymal stem cell-derived TGF-beta. J Immunol. 2010; 184:5885–94. [PubMed: 20382885]
12. Rameshwar P. Breast cancer cell dormancy in bone marrow: potential therapeutic targets within the marrow microenvironment. Exp. Rev Anticancer Ther. 2010; 10:129–32.
13. Comsa S, Ciuculescu F, Raica M. Mesenchymal stem cell-tumor cell cooperation in breast cancer vasculogenesis. Mol Med Report. 2012; 5:1175–80.
14. Feng B, Chen L. Review of mesenchymal stem cells and tumors: executioner or coconspirator? Cancer Biother Radiopharm. 2009; 24:717–21. [PubMed: 20025552]
15. Greco SJ, Rameshwar P. Microenvironmental considerations in the application of human mesenchymal stem cells in regenerative therapies. Biologics. 2008; 2:699–705. [PubMed: 19707450]
16. Riggi N, Suva ML, De VC, et al. EWS-FLI-1 modulates miRNA145 and SOX2 expression to initiate mesenchymal stem cell reprogramming toward Ewing sarcoma cancer stem cells. Genes Dev. 2010; 24:916–32. [PubMed: 20382729]
17. De BA, Narine K, De NW, et al. Resident and bone marrow-derived mesenchymal stem cells in head and neck squamous cell carcinoma. Oral Oncol. 2010; 46:336–42. [PubMed: 20219413]
18. Corcoran KE, Trzaska KA, Fernandes H, et al. Mesenchymal stem cells in early entry of breast cancer into bone marrow. PLos One. 2008; 3:e2563. [PubMed: 18575622]
19. Mishra PJ, Mishra PJ, Humeniuk R, et al. Carcinoma-associated fibroblast-like differentiation of human mesenchymal stem cells. Cancer Res. 2008; 68:4331–9. [PubMed: 18519693]
20. Patel SA, Ramkissoon SH, Bryan M, et al. Delineation of breast cancer cell hierarchy identifies the subset responsible for dormancy. Sci Rep. 2012; 2
21. Jadidi-Niaragh F, Mirshafiey A. The deviated balance between regulatory T cell and Th17 in autoimmunity. Immunopharmacol Immunotoxicol. 2012; 34:727–39. [PubMed: 22316060]
22. Gnerlich JL, Mitchem JB, Weir JS, et al. Induction of Th17 cells in the tumor microenvironment improves survival in a murine model of pancreatic cancer. J Immunol. 2010; 185:4063–71. [PubMed: 20805420]
23. Valmori D, Raffin C, Raimbaud I, et al. Human RORt+ TH17 cells preferentially differentiate from naive FOXP3+ TC_{reg} in the presence of lineage-specific polarizing factors. ProcCNatl Acad Sci. 2010; 107:19402–7.
24. Wainwright DA, Sengupta S, Han Y, et al. The presence of IL-17A and T helper 17 cells in experimental mouse brain tumors and human glioma. PLos One. 2010; 5:e15390. [PubMed: 21060663]

25. Mantel, PY.; Schmidt-Weber, C. Transforming growth factor-beta: Recent advances on its role in immune tolerance.. In: Cuturi, MC.; Anegon, I., editors. Suppression and Regulation of Immune Responses. Humana Press; 2011. p. 303-38.
26. Maruyama T, Kono K, Mizukami Y, et al. Distribution of Th17 cells and FoxP3(C) regulatory T cells in tumor-infiltrating lymphocytes, tumor-draining lymph nodes and peripheral blood lymphocytes in patients with gastric cancer. Cancer Sci. 2010; 101:1947–54. [PubMed: 20550524]
27. Zhang Y, Ma D, Zhang Y, et al. The imbalance of Th17/T_{reg} in patients with uterine cervical cancer. Clin Chimca Acta. 2011; 412:894–900.
28. Tong Z, Yang XO, Yan H, et al. A protective role by interleukin-17F in colon tumorigenesis. PLos One. 2012; 7:e34959. [PubMed: 22509371]
29. Rameshwar P, Denny TN, Stein D, et al. Monocyte adhesion in patients with bone marrow fibrosis is required for the production of fibrogenic cytokines. Potential role for interleukin-1 and TGF-beta. J Immunol. 1994; 153:2819–30. [PubMed: 7521370]
30. Potian JA, Aviv H, Ponzio NM, et al. Veto-like activity of mesenchymal stem cells: Functional discrimination between cellular responses to alloantigens and recall antigens. J immunol. 2003; 171:3426–34. [PubMed: 14500637]
31. Lim PK, Bliss SA, Patel SA, et al. Gap junction-mediated import of microRNA from bone marrow stromal cells can elicit cell cycle quiescence in breast cancer cells. Cancer Res. 2011; 71:1550–60. [PubMed: 21343399]
32. Rao G, Patel PS, Idler SP, et al. Facilitating role of preprotachykinin-I gene in the integration of breast cancer cells within the stromal compartment of the bone marrow: A Model of Early Cancer Progression. Cancer Res. 2004; 64:2874–81. [PubMed: 15087406]
33. Park JM, Munoz JL, Won BW, et al. Exogenous CXCL12 activates protein kinase C to phosphorylate connexin 43 for gap junctional intercellular communication among confluent breast cancer cells. Cancer Lett. 2013; 331:84–91. [PubMed: 23262036]
34. Greco SJ, Patel SA, Bryan M, et al. AMD3100-mediated production of interleukin-1 from mesenchymal stem cells is key to chemosensitivity of breast cancer cells. Am J Cancer Res. 2011; 1:701–15. [PubMed: 22016821]
35. Montesinos JJ, Mora-Garcia MD, Mayani H, et al. In vitro evidence of the presence of mesenchymal stromal cells in cervical cancer and their role in protecting cancer cells from cytotoxic T cell activity. Stem Cells Dev. 2013; 22:2508–19. [PubMed: 23656504]
36. Rattigan Y, Hsu JM, Mishra PJ, et al. Interleukin 6 mediated recruitment of mesenchymal stem cells to the hypoxic tumor milieu. Exp Cell Res. 2010; 316:3417–24. [PubMed: 20633553]
37. Rhodes L, Antoon J, Muir S, et al. Effects of human mesenchymal stem cells on ER-positive human breast carcinoma cells mediated through ER-SDF-1/CXCR4 crosstalk. Mol Cancer. 2010; 9:295. [PubMed: 21087507]
38. Hattermann K, Mentlein R. An Infernal Trio: The chemokine CXCL12 and its receptors CXCR4 and CXCR7 in tumor biology. Ann Anatomy. 2013; 195:103–10.
39. Sharma MB, Limaye LS, Kale VP. Mimicking the functional hematopoietic stem cell niche in vitro: recapitulation of marrow physiology by hydrogel-based three-dimensional cultures of mesenchymal stromal cells. Haematologica. 2012; 97:651–60. [PubMed: 22058199]
40. Uy GL, Rettig MP, Motabi IH, et al. A phase 1/2 study of chemosensitization with the CXCR4 antagonist plerixafor in relapsed or refractory acute myeloid leukemia. Blood. 2012; 119:3917–24. [PubMed: 22308295]
41. Lin G, Wang J, Lao X, et al. Interleukin-6 inhibits regulatory T cells and improves the proliferation and cytotoxic activity of cytokine-induced killer cells. J Immunother. 2012; 35:337–43. [PubMed: 22495391]

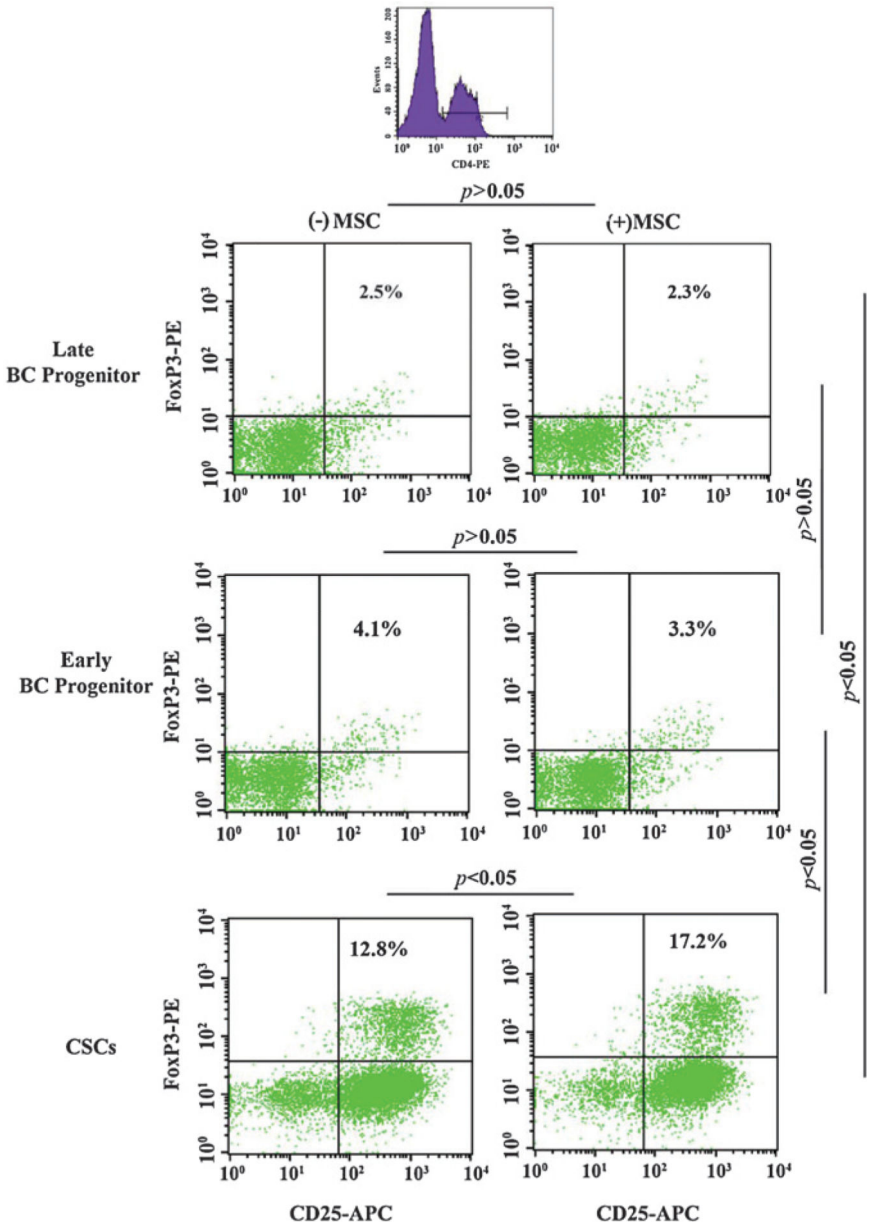

Figure 1. Relative T_{reg} induction in co-cultures with different BCC subsets and MSCs

PBMCs were co-cultured with different BCC subsets in the presence or absence of autologous MSCs. After five days, the PBMCs were labeled with FITC-conjugated anti-CD4, APC-conjugated anti-CD25, and PE-conjugated anti-FoxP3. T_{reg} frequency was assessed by flow cytometry by gating the CD4(+) cells. Figure represents six experiments, each performed with a different donor.

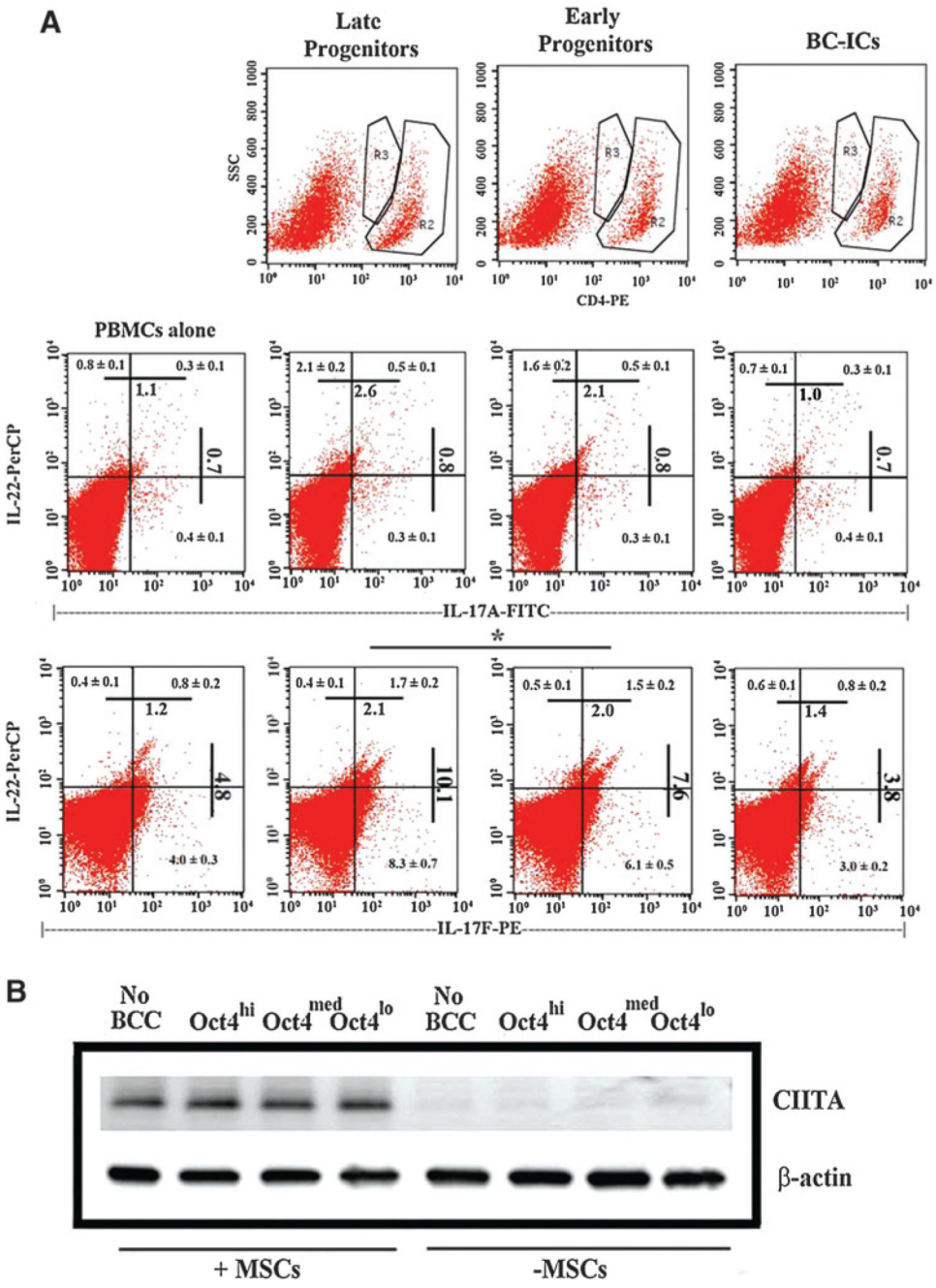

Figure 2. Analyses for intracellular Th17-associated cytokines and western blot for CTLA-4

(A) PBMCs were cultured with different BCC subsets and autologous MSCs. After 5 days, cells were labeled with anti-CD4, anti-IL-17A, anti-IL-17F, and anti-IL-22. The upper panels show the populations that were gated for further analyses. The middle panels depict IL-17A and IL-22 expression; the lower panels depict IL-17F and IL-22 expressions. The Figure represents six experiments, each performed with MSCs and PBMCs from a different donor. Each quadrant shows the mean% ± SD.

(**B)** Whole cell extracts from the PBMCs selected in the cultures described in 'A' were studied for CTLA-4 by western blot.

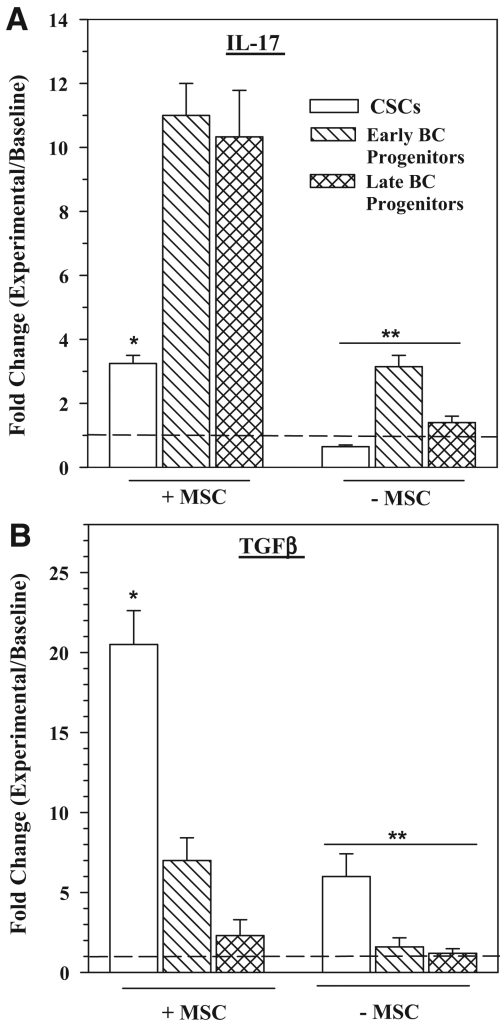

Figure 3. IL-17 and bioactive TGFβ1 production in co-cultures with different BCC subsets and MSCs

PBMCs were cultured with different BCC subsets in the presence or absence of MSCs. At day 4, the media were collected and then quantitated for IL-17 by ELISA and bioactive TGFβ1. The results are presented as the mean ± SD (n = 4) fold change over the values for PBMCs alone (baseline). * $p < 0.01$ vs. early and late progenitors. ** $p < 0.01$ vs. equivalent experimental points with MSCs.

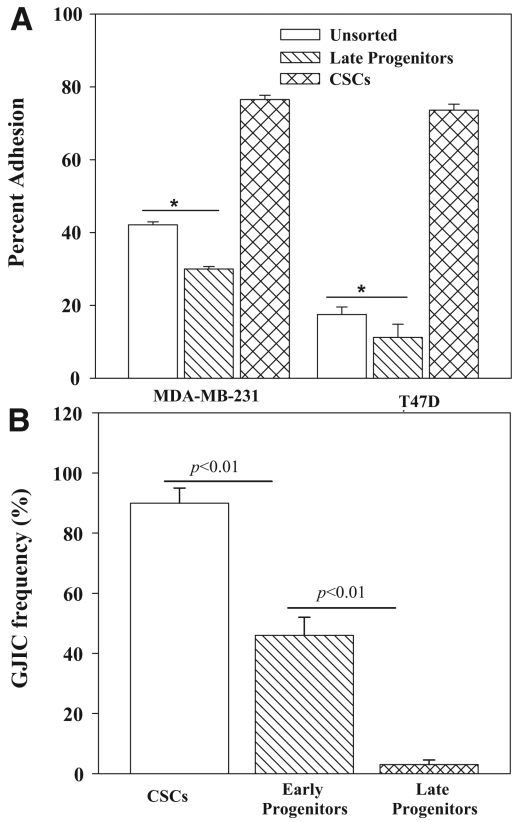

Figure 4. Interaction between MSCs and BCC subsets

(A) Unsorted BCCs, CSCs and late BC progenitors were studied for adherence to MSCs by a fluorescence based method (see Methods section). The results are presented as the % adherence to MSCs, mean ± SD, n = 4. **(B)** GJIC was assessed between MSCs and CFDA-labeled BCC subsets. The method is described in Materials and Methods. The transfer of CFDA to MSCs was assessed by fluorescence microscopy using the $EVOS_{fl}$ imager and by immunofluorescence. The data were comparable and are presented together as the % GJIC ± SD, n = 4.

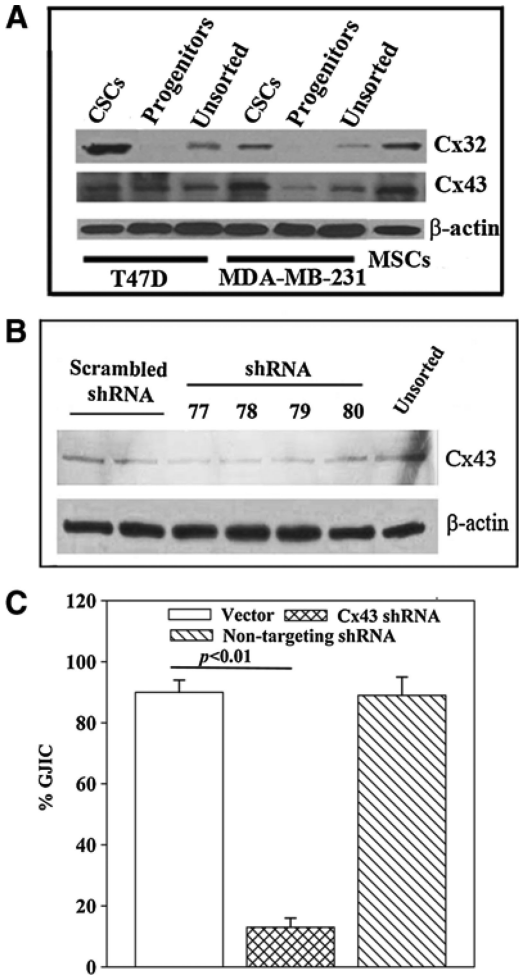

Figure 5. Role of Cx43 in GJIC between CSCs and MSCs

(A) Whole cell extracts from unsorted BCCs, CSCs and BC progenitors from MDA-MB-231 and T47D were studied for Cx32 and Cx43 by western blots. The membranes were stripped and reprobed for β-actin. **(B)** Whole cell extracts from CSCs (MDA-MB-231), transfected with different Cx43 shRNA sequences, were studied for Cx43 by western blot. The membrane was stripped and reprobed for β-actin. **(C)** Dye transfer assay for GJIC was performed with CSCs, transfected with backbone vector, Cx43 shRNA-77 or non-targeting shRNA. The data are presented as the % GJIC ± SD, n = 4.

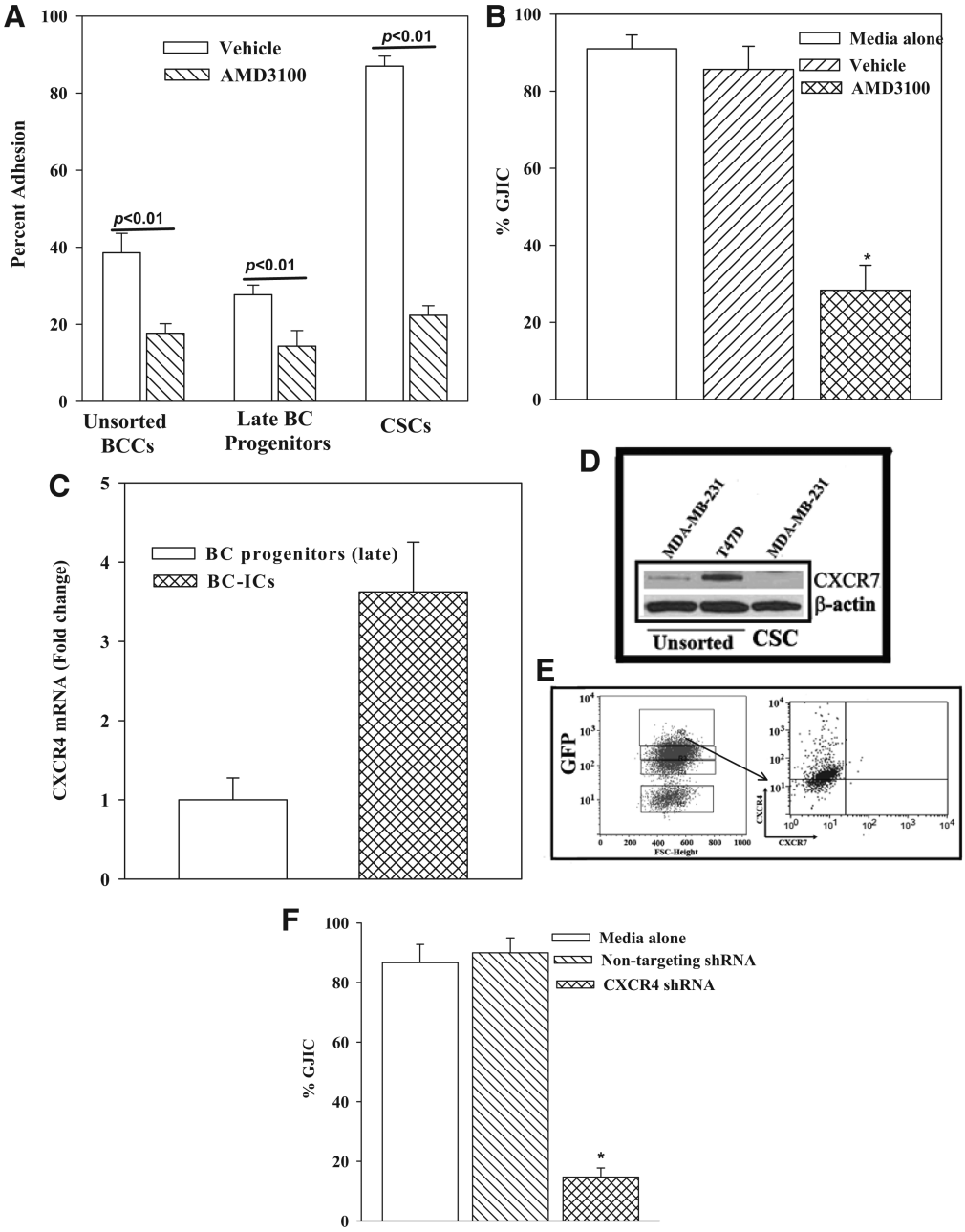

Figure 6. Effect of CXCR4 in the adherence between CSCs and MSCs

(A) Adherence between BCC subsets and MSCs was performed in the presence of 100 ng/mL AMD3100 or vehicle. The % adherence is presented as mean ± SD, n = 4. **(B)** GJIC was studied with CFDA-labeled CSCs and MSCs, in the presence of 100 ng/mL AMD3100. Controls contained vehicle or media alone. The % GJIC is presented as mean ± SD, n = 4. **(C)** Real time PCR was per formed for CXCR4 using total RNA from BC progenitors and CSCs. The values for BC progenitors were assigned values of 1. The values for CSCs are presented as fold change in CXCR4 mRNA over BC progenitors. **(D)** Western blots were performed for CXCR7 with unsorted T47D and MDA-MB-231, and CSCs from MDA-MB-231. The membranes were stripped and reprobed for β-actin. **(E)** The top 5% GFP cells

of MDA-MB-231 ($Oct4^{hi}$) (left panel) were gated and then analyzed for CXCR4 and CXCR7 by flow cytometry (right panel). **(F)** The role of CXCR4 in GJIC between CSCs and MSCs was studied by dye exchange. The CSCs were knocked down for CXCR4 or transfected with a non-targeting shRNA. Baseline GJIC was assessed in cultures with media alone. * $p < 0.01$ vs. media alone and non-targeting shRNA.

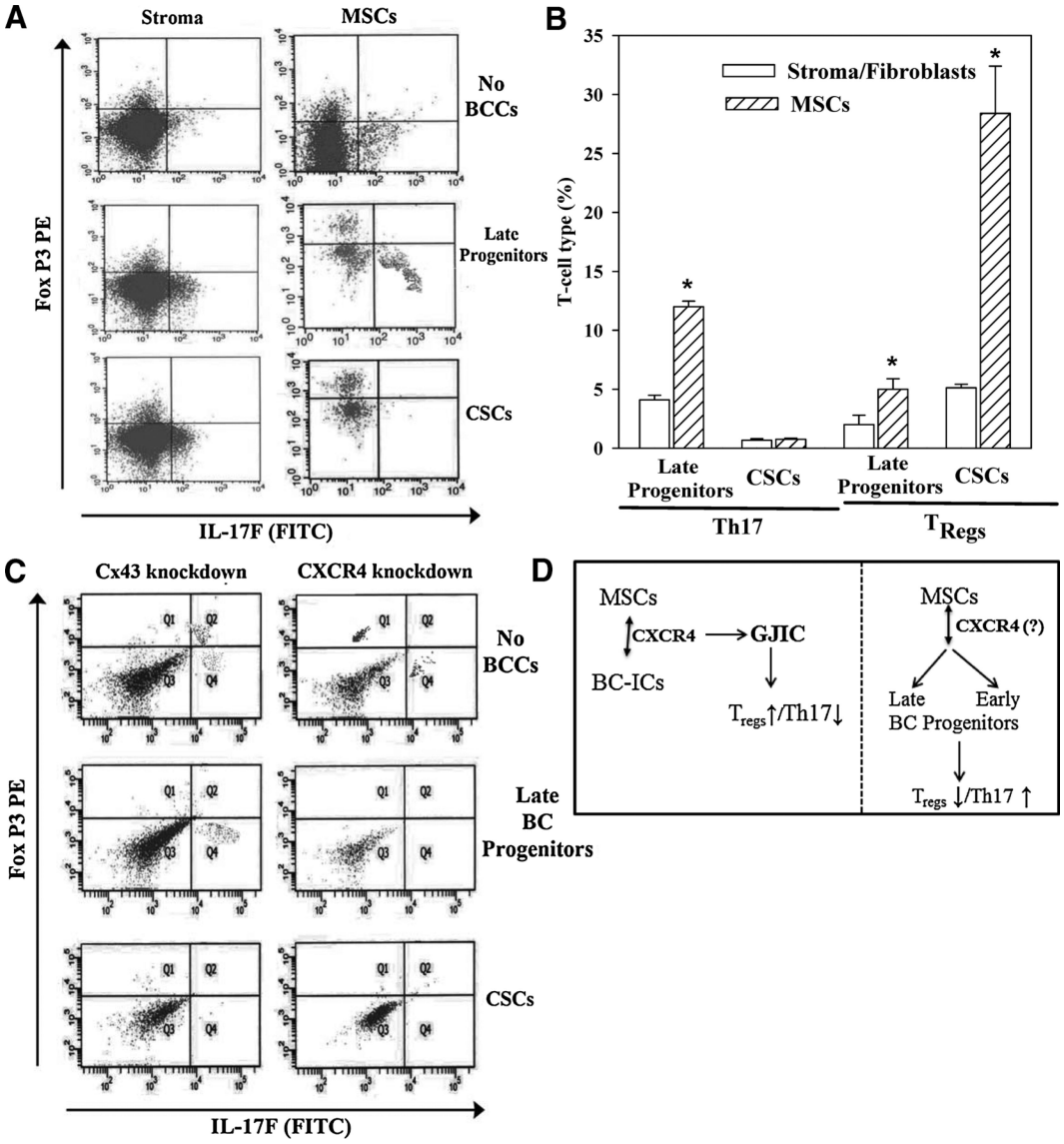

Figure 7. Specificity of MSCs, Cx43 and CXCR4 in T-cell polarization

(A) PBMCs were cultured with different BCC subsets and autologous BM stroma (fibroblasts) or MSCs. After 5 days, cells were labeled with anti-CD4, anti-IL-17A and anti-FoxP3. The Figure represents six experiments, each performed with autologous stroma and PBMCs from a different donor. **(B)** Shown are the mean % changes in Th17 and T_{regs} in autologous PBMCs and MSCs or stroma, ± SD, n = 6. **(C)** PBMCs were co-cultured with MSCs and different BCC subsets, knockdown for *Cx43* or *CXCR4*. The CD4+ cells were gated and then analyzed for FoxP3 and IL17A. The Figure represents four experiments, each performed with cells from a different donor. **(D)** Diagram summarizing the key findings. Left panel: MSCs interact with CSCs with the involvement of CXCR4, resulting in GJIC, increased T_{reg} and decreased Th17. Right panel: In the presence of late and early BC progenitors, MSCs induced Th17 response with concomitant decrease in T_{reg}. It was unclear what role CXCR4 has in the interaction between MSCs and the BC progenitors.